

Copyright 2020 Society of Photo-Optical Instrumentation Engineers.
One print or electronic copy may be made for personal use only.
Systematic reproduction and distribution, duplication of any material
in this paper for a fee or for commercial purposes, or modification of
the content of the paper are prohibited.

Colombo, L., Samaei, S., Lanka, P., Ancora, D., Pagliuzzi, M.,
Durduran, T., ... & Pifferi, A. (2021, March). Speckle fluctuations in
time-domain diffuse optics. In *Dynamics and Fluctuations in
Biomedical Photonics XVIII* (Vol. 11641, p. 116410J). International
Society for Optics and Photonics.

<https://doi.org/10.1117/12.2577622>

Speckle fluctuations in time-domain diffuse optics

Lorenzo Colombo,^{1,*} Saeed Samaei,² Pranav Lanka,¹ Daniele Ancora,¹ Marco Pagliuzzi,³ Turgut Durduran,^{3,4} Piotr Sawosz,² Adam Liebert,² and Antonio Pifferi^{1,5}

1) Politecnico di Milano, Dipartimento di Fisica, Milano, Italy 2) Nalecz Institute of Biocybernetics and Biomedical Engineering, Polish Academy of Sciences, Warsaw, Poland 3) ICFO—Institut de Ciències Fotòniques, The Barcelona Institute of Science and Technology, Castelldefels (Barcelona), Spain 4) Institució Catalana de Recerca i Estudis Avançats (ICREA), Barcelona, Spain 5) Istituto di Fotonica e Nanotecnologie, Consiglio Nazionale delle Ricerche (CNR), Milano, Italy

ABSTRACT

Time-domain diffuse optics exploits near infrared light pulses diffused in turbid samples to retrieve their optical properties e.g., absorption and reduced scattering coefficients. Usually, the detected fields are not affected by light coherence, thus the photon diffusion equation can be used to interpret the data. However, speckle effects are exploited in several techniques e.g., diffuse correlation spectroscopy (DCS), to retrieve information regarding the tissue dynamics. Here, using a highly coherent Ti:Sapphire mode-locked laser and a single-mode detection fiber, we report the direct observation of temporal fluctuations in the measured distribution of time-of-flights (DTOF) curve. We study the dependence of these fluctuations on the sample dynamical properties (moving from fluid to rigid tissue-mimicking phantoms) and on the area of the detection fiber, which is directly linked to the number of collected modes/coherence areas. For studying the statistical properties of the observed fluctuations, we introduced a specific parameter for its quantification. We verified that the observed effect is compatible with speckle fluctuations, thus interpreting it as a time-resolved speckle pattern. By providing physical insights on light propagation in random media, our observation may enable the simultaneous monitoring of the tissue optical and dynamical properties.

Keywords: time-domain diffuse optics, diffusive media, speckle fluctuations.

*lorenzo.colombo@polimi.it

1. INTRODUCTION AND METHODS

Time-domain (TD) diffuse optics is a non-invasive optical technique which exploits a pulsed light source to measure the optical coefficients of a turbid medium, such as absorption and reduced scattering¹. In TD diffuse optics, interference effects are typically negligible, due to the use of multi-mode fibers for detection of the diffused light which maximize light harvesting. In other diffuse optical techniques, such as in diffuse correlation spectroscopy (DCS), single-mode fibers are used to exploit the effect of light interference (i.e. speckles) for retrieving information regarding the sample dynamics^{2,3}. Following this lines, TD-DCS is a novel spectroscopic technique which aims to measure both the optical properties and the dynamics of a biological tissue. This is achieved by using a highly coherent pulsed laser and measuring the arrival time of each photon.⁴⁻⁷ Here, by using a TD-DCS setup, we report the direct observation of coherent (i.e. speckle) fluctuations in the measured distribution of times-of-flight (DTOF)⁸.

Our TD-DCS setup is based on a Ti:Sapphire mode-locked laser operating at 785 nm. It is tuned to have a pulse width of 200 ps (full-width at half-maximum), a single-photon avalanche photodiode (PDM, MPD srl, Italy), and a time-correlated single-photon counting acquisition board (TimeHarp 260 pico, PicoQuant, Germany). Light is delivered to the sample with a 100 μm core diameter graded-index fiber and collected, in reflectance geometry, at a source-detector separation $\rho = 1.5$ cm with a 5 μm diameter single-mode (SM) fiber (HP780, Thorlabs, Germany). Further details on the setup can be found in Ref 3. For each configuration, the DTOF curves were measured with a sampling time (denoted as macro-time τ) of 100 ms, with a time-of-flight (denoted as micro-time t) resolution of 25 ps. Each experiment had a total duration of 300 s, and a constant input power of 50 mW was used.

To quantify the fluctuations, we define the contrast (C) in the following way: $C(t, \tau) = \left(\frac{R(t, \tau)}{\langle R(t, \tau) \rangle_\tau} \right) - 1$, where $R(t, \tau)$ is the measured DTOF and $\langle R(t, \tau) \rangle_\tau$ denotes the average (over the macro-time) DTOF curve.

2. RESULTS AND DISCUSSION

Figure 1 reports the results for two set of experiments. In the first row we report the measurements with a single-mode fiber and (a) a 5:95 mixture of lipid (Intralipid 20%) in water, with nominal properties $\mu'_s = 10 \text{ cm}^{-1}$ and $\mu_a = 0.02 \text{ cm}^{-1}$ (b) a silicone phantom, with properties $\mu'_s = 10 \text{ cm}^{-1}$ and $\mu_a = 0.05 \text{ cm}^{-1}$, and (c) a solid resin sample with properties $\mu'_s = 18.6 \text{ cm}^{-1}$ and $\mu_a = 0.009 \text{ cm}^{-1}$. In the second row, we report the measurements with another solid resin phantom with optical properties $\mu'_s = 10 \text{ cm}^{-1}$ and $\mu_a = 0.1 \text{ cm}^{-1}$, changing the diameter of the detection fiber: d) $25 \mu\text{m}$ e) $10 \mu\text{m}$ and f) $5 \mu\text{m}$.

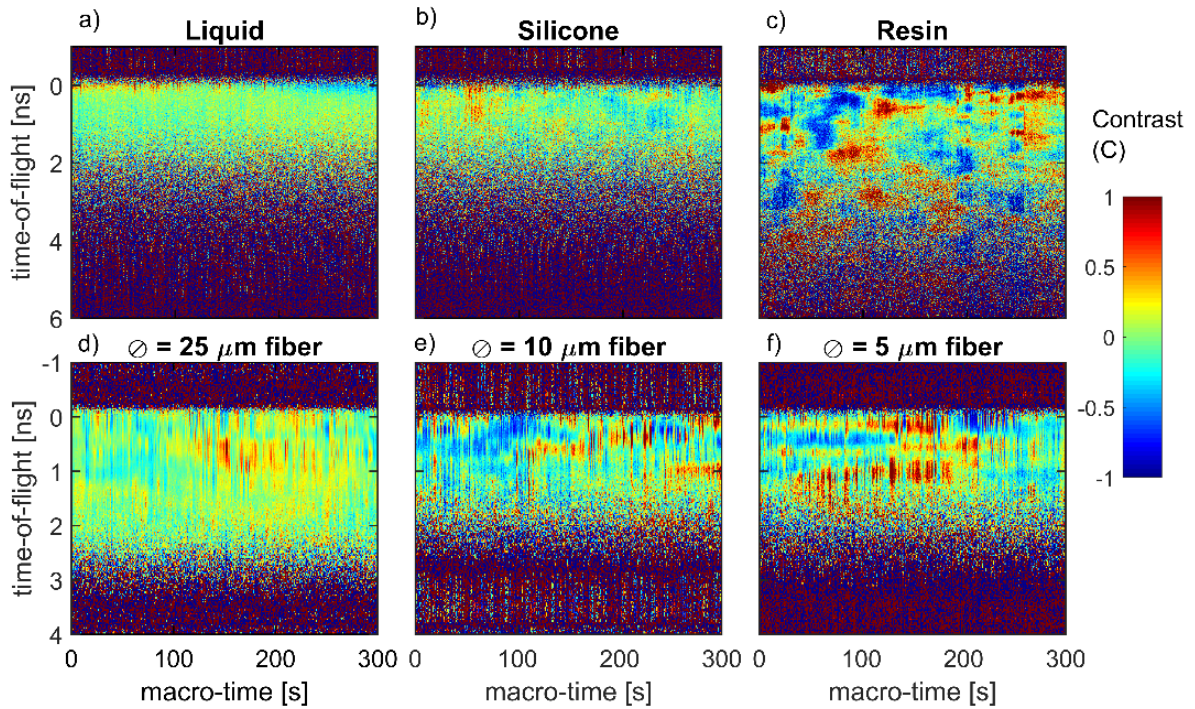


Figure 1: Contrast $C(t, \tau)$ of the DTOF fluctuations (definition in main text). The x-axis is the macro-time τ , the y-axis is the time-of-flight t . We set time $t = 0$ at the peak of the IRF. Top row shows results with a single-mode collection fiber with different phantoms: (a) liquid (b) silicone or (c) resin. Bottom row shows results with a solid resin phantom with different collection fiber diameters: (d) 25 (e) 10 or (f) 5 μm .

When using a single mode collection fiber, as in Figure 1 top row, the measured fluctuations strongly depend on the sample stiffness. The visibility, quantified by the contrast $C(t, \tau)$, increases from the fluid to the resin one, due to a reduced self-averaging effect. The bottom row of Figure 1 shows also that the measured fluctuations appear only when the number of collected modes approaches unity: due to the reduction in the detection fiber diameter, the effect of spatial averaging disappears.

In order to quantitatively describe our observations, we adapted the theory developed by Goodman which describes the statistical properties of speckle intensity⁹. By assuming the detection as

a Poissonian process and that the measured intensity determined by the interference of many independent photon paths, the variance of the resulting intensity $\sigma_I^2(t)$ can be written as:

$$\sigma_I^2(t) = \langle I(t) \rangle + \beta(t) \langle I(t) \rangle^2. \quad (1)$$

Here, the $\langle I(t) \rangle$ is the average intensity at a given time-of-flight t and $\beta(t)$ is the corresponding value of the coherence parameter, which depends on the number of detected modes and the source coherence properties¹⁰. For unpolarized detection, its ideal value is 0.5. We tested our hypothesis by measuring a solid resin phantom, with nominal optical properties $\mu'_s = 4.7 \text{ cm}^{-1}$ and $\mu_a = 0.06 \text{ cm}^{-1}$, under three different pulse durations, which result in different coherence levels. The corresponding instrument response function (IRF)¹¹ full width at half-maximum (FWHM) was 450 ps, 225 ps and 175 ps. After the acquisition, we computed the intensity auto-correlation g_2 by considering 100ps-wide gates and 100 ms sampling time. In Fig. 2 we compare the value of the $\beta(t)$ parameter measured from the amplitude of the intensity auto-correlation $g_2(t, \tau)$, with its value predicted using Eq. (1) and the measured DTOF intensity fluctuations. From Fig. 2, we might see that $\beta(t)$ retrieved using speckle theory agrees well with the measured one for all the pulse durations considered.

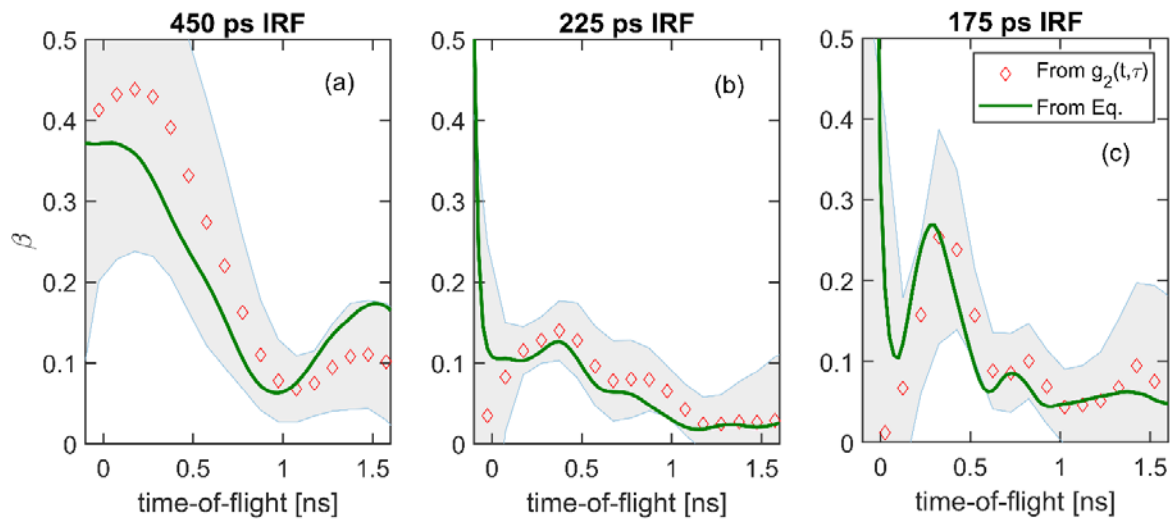


Figure 2: Measured β parameter in a solid resin phantom experiment, for three different IRF FWHM: a) 450 ps, b) 225 ps and c) 175 ps. The red diamonds show the β parameter retrieved from the amplitude of the intensity auto-correlation $g_2(t, \tau)$, considering 100 ps wide gates, with the gray shaded region reporting the standard deviation over 5 minutes of acquisition. The green line reports the β retrieved from Eq. 1 using the measured DTOF fluctuations.

Finally, we tested whether the effect was detectable also in an in vivo experiment. In particular, in Fig. 3 we report the results of an arterial occlusion (250 mmHg pressure) on the forearm of an adult subject. In the upper plot of Fig. 3, we report the raw intensity time trace during the protocol. The occlusion was performed from minute 2 to minute 5. We notice that the intensity variability strongly increased during the occlusion, returning to its baseline value a few minutes after the release.

In order to quantify the intensity fluctuations, we define the squared speckle contrast as follows¹²:

$$k^2 = \frac{\sigma_I^2 - \langle I \rangle^2}{\langle I \rangle^2}, \quad (2)$$

where the symbols have the same meaning of Eq. (1). In Fig. 3, lower plot, we report the reciprocal of the measured speckle contrast k^2 , normalized to its baseline value. We might see that the retrieved time trace is consistent with the expected blood flow trend. Its value is strongly reduced during the occlusion (minute 2) and shows a typical hyperemic peak immediately after the release (minute 5).

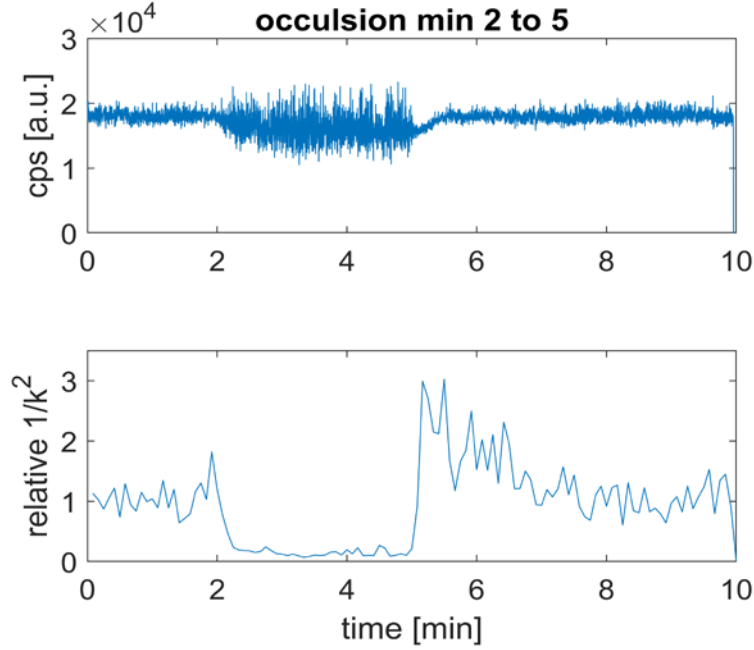


Figure 3: In vivo experiment: arterial occlusion protocol on the forearm of an adult subject. The occlusion, with 250 mmHg pressure, was performed from minute 2 to minute 5. In the upper plot, we report the measured intensity trace (in counts per second) with a sampling time of 100 ms. On the lower plot, we show the reciprocal of the retrieved speckle contrast, normalized to baseline. The resulting trace has a temporal evolution which agrees well with the expected blood flow trend.

To summarize, in this work we have reported the first direct observation of speckle fluctuations in time-domain diffuse optics. We highlight that the observed fluctuations are present even after few cm of propagation in the turbid medium. The effect has a strong dependence on the sample dynamical properties and on the number of detected modes. Since it agrees with classical speckle theory, it can be interpreted a temporal speckle effect/pattern. Finally, we detected it also in an in vivo experiment, and we proposed a simple metric for linking it to blood flow variations. However, further investigations are ongoing for an accurate quantification of blood flow from the measured intensity fluctuations.

ACKNOWLEDGMENTS: The authors acknowledge financial support from the European Union's H2020 programs LASERLAB EUROPE V (n. 871124) and LUCA (n. 688303, H2020-ICT-2015), Marie Skłodowska-Curie Action HI-PHRET (n. 799230) and Marie Skłodowska-Curie Innovative Training Network BITMAP (n. 675332).

REFERENCES

- [1] Torricelli, A., Contini, D., Pifferi, A., Caffini, M., Re, R., Zucchelli, L. and Spinelli, L., “Time domain functional NIRS imaging for human brain mapping,” *Neuroimage* (2014).
- [2] Boas, D. A. and Yodh, A. G., “Spatially varying dynamical properties of turbid media probed with diffusing temporal light correlation,” *J. Opt. Soc. Am. A* **14**(1), 192–215 (1997).
- [3] Durduran, T., Choe, R., Baker, W. B. and Yodh, A. G., “Diffuse optics for tissue monitoring and tomography,” *Reports Prog. Phys.* **73**, 076701 (2010).
- [4] Sutin, J., Zimmerman, B., Tyulmankov, D., Tamborini, D., Wu, K. C., Selb, J., Gulinatti, A., Rech, I., Tosi, A., Boas, D. A. and Franceschini, M. A., “Time-domain diffuse correlation spectroscopy,” *Optica* **3**(9), 1006 (2016).
- [5] Pagliazzi, M., Sekar, S. K. V., Colombo, L., Martinenghi, E., Minnema, J., Erdmann, R., Contini, D., Mora, A. D., Torricelli, A., Pifferi, A. and Durduran, T., “Time domain diffuse correlation spectroscopy with a high coherence pulsed source: in vivo and phantom results,” *Biomed. Opt. Express* **8**(11), 5311 (2017).
- [6] Pagliazzi, M., Sekar, S. K. V., Di Sieno, L., Colombo, L., Durduran, T., Contini, D., Torricelli, A., Pifferi, A. and Mora, A. D., “In vivo time-gated diffuse correlation spectroscopy at quasi-null source-detector separation,” *Opt. Lett.* **43**(11), 2450 (2018).
- [7] Tamborini, D., Farzam, P., Zimmermann, B., Wu, K.-C., Boas, D. A. and Franceschini, M. A., “Development and characterization of a multidistance and multiwavelength diffuse correlation spectroscopy system,” *Neurophotonics* (2017).
- [8] Colombo, L., Samaei, S., Lanka, P., Ancora, D., Pagliazzi, M., Durduran, T., Sawosz, P., Liebert, A. and Pifferi, A., “Coherent fluctuations in time-domain diffuse optics,” *APL Photonics* (2020).
- [9] Goodman, J. W., “Some Effects of Target-Induced Scintillation on Optical Radar Performance,” *Proc. IEEE* (1965).
- [10] Bellini, T., Glaser, M. A., Clark, N. A. and Degiorgio, V., “Effects of finite laser coherence in quasielastic multiple scattering,” *Phys. Rev. A* **44**(8), 5215–5223 (1991).
- [11] Colombo, L., Pagliazzi, M., Sekar, S. K. V., Contini, D., Mora, A. D., Spinelli, L., Torricelli, A., Durduran, T. and Pifferi, A., “Effects of the instrument response function and the gate width in time-domain diffuse correlation spectroscopy: model and validations,” *Neurophotonics* **6**(03), 1 (2019).
- [12] Bi, R., Dong, J. and Lee, K., “Multi-channel deep tissue flowmetry based on temporal diffuse speckle contrast analysis,” *Opt. Express* **21**(19), 22854 (2013).